Ensemble-based simultaneous state and parameter estimation with MM5

Altuğ Aksoy,[1,2] Fuqing Zhang,[3] and John W. Nielsen-Gammon[3]

Received 1 March 2006; revised 25 April 2006; accepted 9 May 2006; published 16 June 2006.

[1] The performance of the ensemble Kalman filter (EnKF) under imperfect model conditions is investigated through simultaneous state and parameter estimation for a numerical weather prediction model of operational complexity (MM5). The source of model error is assumed to be the uncertainty in the vertical eddy mixing coefficient. Assimilations are performed with a 12-hour interval with simulated sounding and surface observations of horizontal winds and temperature. The mean estimated parameter value nicely converges to the true value within a satisfactory level of variability due to sufficient model sensitivity to parameter uncertainty and detectable (relative to ensemble sampling noise) correlation signal between the parameter and observed variables. **Citation:** Aksoy, A., F. Zhang, and J. W. Nielsen-Gammon (2006), Ensemble-based simultaneous state and parameter estimation with MM5, *Geophys. Res. Lett.*, *33*, L12801, doi:10.1029/2006GL026186.

1. Introduction

[2] In recent years, especially in the atmospheric science community, the ensemble Kalman filter (EnKF) has drawn considerable research attention as an alternative data assimilation technique to the operationally-established four-dimensional variational (4DVAR) method which is currently being operated by the European Centre for Medium-Range Weather Forecasts [*Rabier et al.*, 2000] and Météo-France [*Gauthier and Thépaut*, 2001]. The EnKF, first proposed in the geophysical literature by *Evensen* [1994], has today reached near-operational status at the Canadian Meteorological Centre for large-scale applications [*Houtekamer et al.*, 2005]. At meso- and smaller scales, the feasibility of the method has been investigated by a number of studies [e.g., *Aksoy et al.*, 2005; *Zhang et al.*, 2006; *Tong and Xue*, 2005; *Dowell et al.*, 2004; *Snyder and Zhang*, 2003]. A fairly complete overview of the theory and practical applications of the EnKF are given by *Evensen* [2003], while *Lorenc* [2004] presents a comparison study between the EnKF and 4DVAR techniques.

[3] The application of ensemble-based simultaneous state and parameter estimation is a very new area of investigation in atmospheric sciences. For numerical weather prediction (NWP) purposes, studies by *Aksoy et al.* [2006] (hereinafter referred to as *AZN*), *Hacker and Snyder* [2005], and *Anderson* [2001] have laid the groundwork for the application of the EnKF to relatively low-order models. Their results are very promising. Successful implementation has also been carried out for steady-state climatological modeling purposes [e.g., *Annan et al.*, 2005a, 2005b]. The current study explores the application of the concept to numerical modeling environments of operational complexity. To our knowledge, this is the first such application of its kind and we hope that it will encourage further investigation by the numerical modeling and data assimilation community.

2. Model and Filter Setup

[4] In this study, the Penn State-NCAR fifth-generation nonhydrostatic mesoscale model MM5 [*Dudhia*, 1993] is used to represent the numerical and implementation complexities associated with an operational forecasting system. The horizontal model domain has 55×55 grid points with 36 km spacing, while there are 43 vertical layers. Employed parameterization schemes are the Medium Range Forecast model (MRF) planetary boundary layer (PBL) scheme, the Grell cumulus scheme with the shallow cumulus option, and the simple ice microphysical scheme. The model prognostic variables include the Cartesian velocity components (u, v, w), pressure perturbation (p'), temperature (T), and mixing ratio for water vapor (q) and several other hydrometeor species.

[5] As the dynamical focus of our previous work was on the thermally-forced sea breeze circulation [*AZN*], the model domain in the current study is chosen such that it covers mostly the Southcentral United Stated and the northern half of Gulf of Mexico where such local circulations are very prominent during summer months. Preliminary simulations showed that the sea breeze was sensitive to the vertical mixing parameterization, so observations should contain considerable information regarding vertical mixing. Parameter estimation computations for this study are based on the eddy mixing coefficient (K_c) for the MRF PBL scheme [*Hong and Pan*, 1996]. In order to represent a global uncertainty in this scheme, it is modified such that the final K_c value determined within the scheme is multiplied by a user-defined multiplier, m_c, before the implicit vertical diffusion computation is performed. Thus, for $m_c = 1.0$, the original MRF PBL computation is simply repeated. The resulting variability in m_c imposes a global influence on vertical diffusion. By implementing a global multiplier to K_c, we merely attempt to account for the uncertainties of the many empirical global parameters within the MRF PBL scheme in a cumulative fashion (K_c itself is spatially and temporally variable).

[1]National Center for Atmospheric Research, Boulder, Colorado, USA.
[2]Previously at Department of Atmospheric Sciences, Texas A&M University, College Station, Texas, USA.
[3]Department of Atmospheric Sciences, Texas A&M University, College Station, Texas, USA.

0094-8276/06/2006GL026186

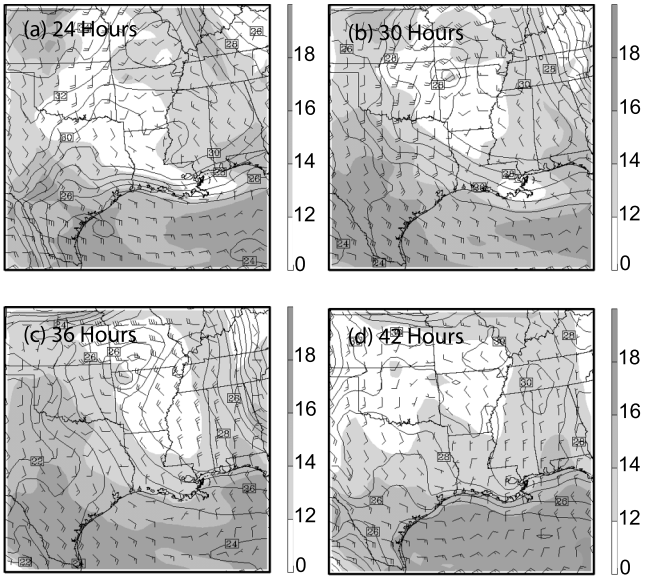

Figure 1. Perfect-model forecast distributions of horizontal wind (full barbs $5ms^{-1}$), temperature (contours of 1.0°C interval), and water vapor mixing ratio (shading with $4gkg^{-1}$ interval) at forecast times (a) 24 hours, (b) 30 hours, (c) 36 hours, and (d) 42 hours at height 0.5 km.

[6] In general, the characteristics of the EnKF are very similar to the filter used in *AZN*. The ensemble has 40 members and is "climatologically initialized" [see *AZN*] using the 40-km NCEP/GCIP analysis for the period 1 June–15 September 2000. Sounding and surface observations of u, v, and T with 324- and 72-km horizontal spacing, respectively, are simulated from a truth simulation (observational errors of $1ms^{-1}$ for u, v and 0.5 K for T). Observations are assimilated every 12 hours and covariance localization using a compactly supported fifth-order correlation function [*Gaspari and Cohn*, 1999] is carried out with a radius of influence of 30 grid points both horizontally and vertically. Finally, at each analysis step, posterior state covariances are "relaxed" to the prior with a ratio of 0.5 as given by *Zhang et al.* [2004], thus forcing the uncertainty in the analysis to be inflated.

3. Spatial Updating of a Global Model Parameter

[7] With the significantly larger number of observations ($\sim 10^3$) in this study compared to *AZN*, contamination of the posterior estimate of m_c by the accumulation of sampling error during the update process becomes an issue. To tackle this problem, a new method, called "spatial updating", is devised that transforms the prior m_c from a scalar to a homogeneous two-dimensional surface array. The updating of the parameter is performed spatially using localization, yielding a spatially-varied posterior distribution. Then, spatial averaging is performed for each ensemble member to obtain the global m_c estimate which is fed into the subsequent forecast cycle. The localization properties employed are the same as for the state variables. In addition, to prevent filter divergence due to parameter variance narrowing, the "conditional covariance inflation" technique of *AZN* is applied with a variance limit set at 1/4 of the initial parameter error.

4. Pure-Forecast Behavior

[8] The 72-hour control ensemble forecast is initialized at 00Z 28 August 2000 (7pm CST which is nearly the peak sea breeze phase) with perfect-model statistics (i.e., the initial true state is taken as one of the ensemble members). With the chosen domain size and resolution, the diurnal signal within the PBL arises both from the sea breeze circulation and the Great Plains low level jet. To illustrate the diurnal signal embedded in the large-scale flow, the horizontal distributions of mean u, v, T, and q are plotted for 24-, 30-, 36-, and 42-hour forecast times at 0.5-km height above surface (Figure 1). A persistent anticyclonic circulation centered near Louisiana is evident at all forecast times. Nevertheless, the impacts of the diurnal circulation are discernible especially across the coastline between East Texas to Louisiana. Specifically, notice the penetration of the temperature and moisture gradients inland from 24 hours (peak sea breeze phase) to 36 hours, the veering of winds to the right during the 24-hour cycle, and the establishment of the northerly return flow due to the land breeze between 36–42 hours.

[9] To analyze the overall strength of correlation between observed variables and m_c, a 72-hour forecast experiment is

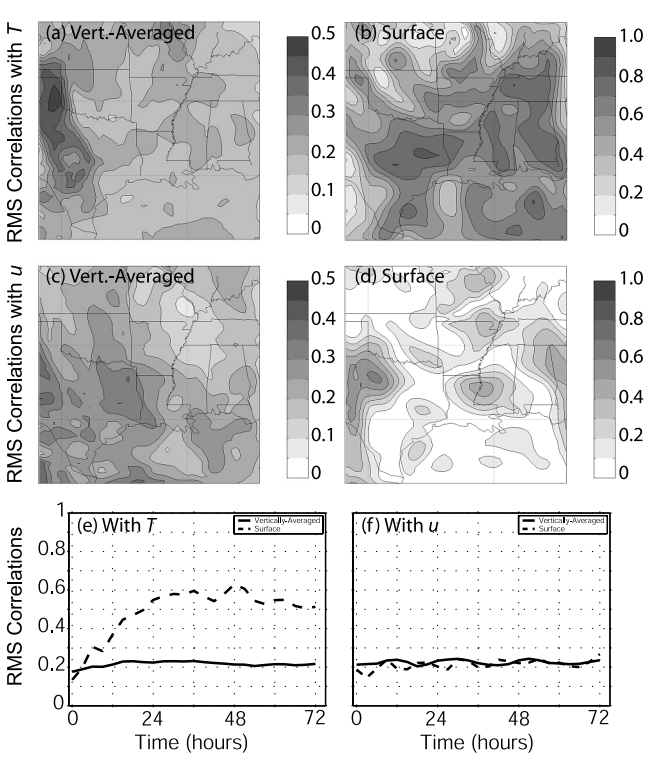

Figure 2. (a–d) Horizontal distribution of vertically-averaged (Figures 2a and 2c) and surface (Figures 2b and 2d) rms correlation between the parameter m_c and the observed variables T (Figures 2a and 2b) and u (Figure 2c and 2d) at the forecast time 24 hours. (e and f) 72-hour evolution of vertically-averaged (solid) and surface (dashed) rms correlation. Contour interval in the spatial distribution plots is 0.05 for Figures 2a and 2c and 0.1 for Figures 2b and 2d.

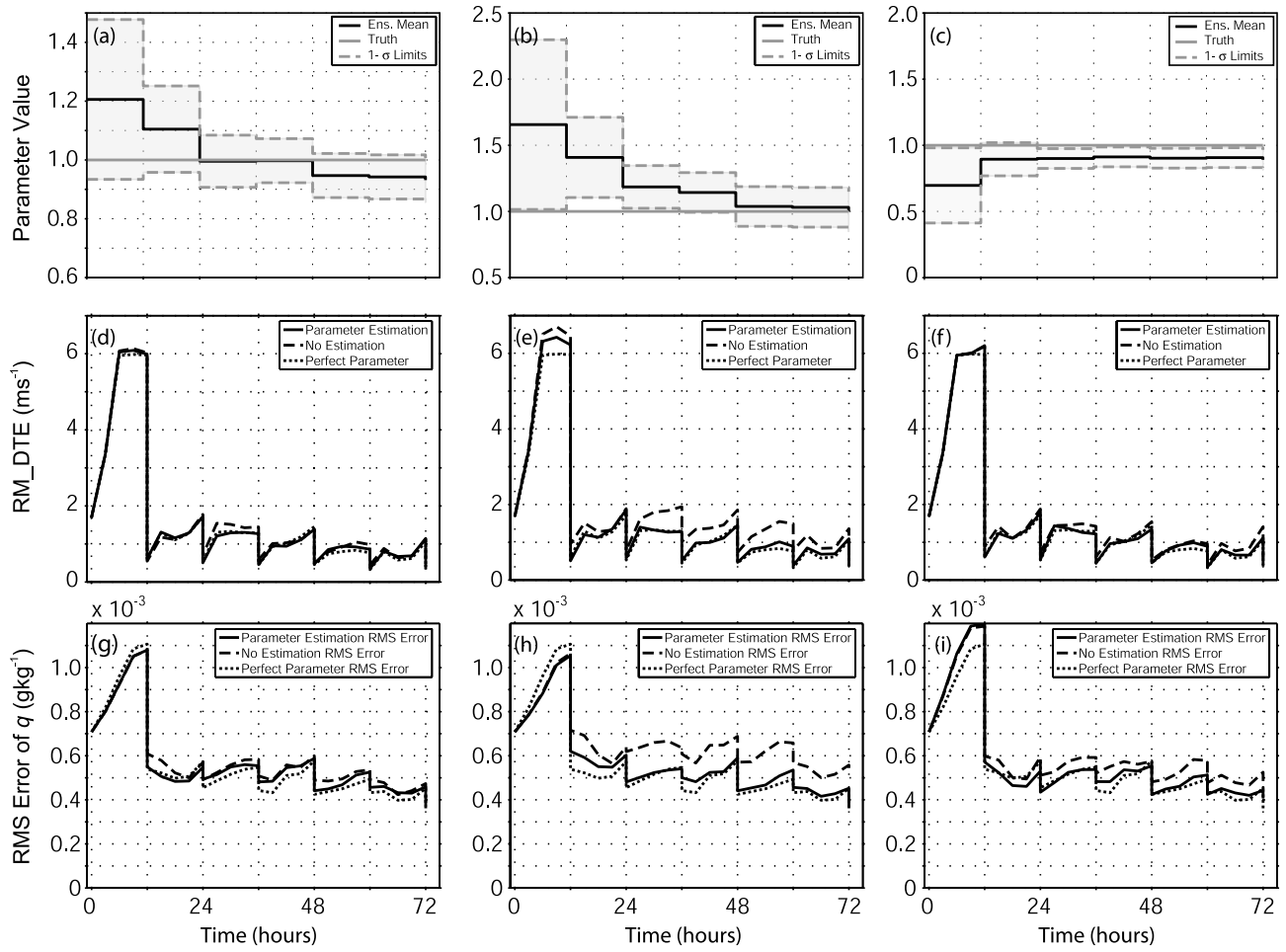

Figure 3. (a–c) The time evolution of estimated mean m_c (solid black) vs. true m_c (solid gray) for initial values of 1.2 (Figure 3a), 1.65 (Figure 3b), and 0.7 (Figure 3c). The shaded area represents the 1−σ limits of m_c spread. (d–i) The time evolution of RM_DTE (Figures 3d–3f) and rms error of q (Figures 3g–3i) for initial m_c values of 1.2 (Figures 3d and 3g), 1.65 (Figures 3e and 3h), and 0.7 (Figures 3f and 3i). Respective quantities from respective no-estimation (perfect-parameter) experiments are shown with dashed (dotted) lines.

carried out with m_c perturbed about the value 1.0 with a standard deviation of 0.3 and the behavior of the root-mean square (rms) correlation ($\bar{r}$) of m_c with prognostic variables is analyzed as in *AZN*. The spatial plot of $\bar{r}$ (computed at the surface and averaged vertically) with T and u at the 24-hour forecast time (Figures 2a–2d) reveals a horizontally- and vertically-varied distribution which is an indication that model dynamics contributes to the evolution of the correlation between the observed variables and m_c. From the 72-hour evolution of the vertically-averaged and surface $\bar{r}$ (Figures 2e–2f), it can be seen that vertically-averaged $\bar{r}$ values consistently stay between 0.2–0.3, which, according to previous findings of *AZN*, appear to be sufficient for parameter identifiability.

5. Parameter Estimation Results

[10] Three 72-hour estimation experiments are carried out with mean initial m_c values of 1.2, 1.65, and 0.7 vs. a true value of 1.0. The time evolution of the estimated mean m_c, along with the true value and the one-standard-deviation (1−σ) spread limits, are shown in Figures 3a–3c. In all 3 experiments, we see that the estimated m_c value consistently converges to the truth, remaining inside or very close to the 1−σ limits most of the time, meeting our basic criterion for estimation performance [*AZN*]. We should also note that the spatial variability in the estimated values of m_c remain within 50% of the initial parameter spread and thus mostly realistic (not shown).

[11] To analyze the impacts of parameter estimation on the state analysis, the time evolution of root-mean difference total energy (RM_DTE) and q rms error within the PBL (surface to 850 hPa) are plotted in Figure 3d–3i [where DTE = $\frac{1}{2}(u' + v' + kT')$, primes denote differences between any two simulations, $k = C_p/T_r$, C_p = 1004.7 Jkg^{-1}K^{-1}, and T_r = 270 K]. For comparison, results from the respective no-estimation (same respective initial m_c error but no estimation of m_c) and perfect-parameter (no m_c error and only state estimation) benchmarks are also plotted. We see that in all 3 experiments, the evolution of the error is stable while the overall error is lower compared to the no-estimation benchmark. The improvement in error becomes distinctly more pronounced for the largest initial m_c error of 0.65. For this case, the overall level of error is ∼14% lower than the no-estimation benchmark and is almost indistinguishable from the perfect-parameter benchmark. Meanwhile, the average

error reduction at analysis steps is also better by ~9%. These metrics are similar but somewhat less impressive when computed over the entire domain depth (not shown). This is not surprising as variations in m_c mainly influence the PBL.

[12] A possible explanation for the observed difference of behavior between the smaller and larger initial parameter errors is linked to the interaction between uncertainties associated with initial conditions and model error. In the specific configuration adopted here, it appears that the initial-state uncertainty may span a sufficiently high-dimensional phase space to also account for the limited model error uncertainty generated through the initial perturbation of the parameter m_c.

[13] The existence of a level of parameter uncertainty to which error growth is not very responsive also suggests that such behavior can possibly be utilized to "calibrate" for the acceptable level of parameter variability. For m_c, the initial spread of ~0.2–0.3 appears not to significantly contribute to the forecast error and hence is within the acceptable level, although a more complete analysis of the associated uncertainty space is necessary.

6. Conclusions

[14] This article explores the use of an EnKF for simultaneous state and parameter estimation with a numerical model of operational complexity (MM5) in an otherwise perfect-model framework. The uncertain model parameter is the multiplier of the eddy mixing coefficient in the MRF PBL scheme. Our satisfactory retrieval of the true parameter value is significant from several points of view. First and foremost, it shows that a sufficiently strong flow-dependent covariance structure is present between observed variables and the estimated parameter, suggesting the prospect of treatment of model error for operational data assimilation through ensemble-based parameter estimation. The ability to retrieve parameter values is also valuable for the testing and validation of the many model parameters, values of which are normally obtained empirically or by trial-and-error. Improvement of numerical models, in this respect, has a direct consequence for deterministic weather forecasting where it is not possible to account for model uncertainties through the probabilistic ensemble approach.

[15] The introduced "spatial updating" of global parameters is observed to contribute substantially to the performance of the estimation process. *AZN* argued that a unified "meta-localization" approach for the simultaneous state and parameter estimation might prove necessary for complex numerical models. We believe that our method of spatial updating, although ad hoc in nature, is one step forward toward this goal, primarily because the spatial information content of observations and the advantages of localization are now being realized. However, the theoretical implications of this procedure on the correlation space itself and if and how convergence properties can be improved are not addressed in this study.

[16] Finally, because of the complexities of the problem on hand, this study has been limited in scope to the estimation of a global scalar parameter. Important considerations such as temporal and spatial variability of parameters have necessarily been left as open scientific questions. We nevertheless believe that our conditional covariance inflation and spatial updating techniques will be well suited for such more generalized estimation problems.

[17] **Acknowledgments.** This research is part of the first author's Ph.D. dissertation sponsored by GTRI/HARC Grant Project H24-2003 and NSF grant ATM-0205599 awarded to the Texas A&M University.

References

Aksoy, A., F. Zhang, J. W. Nielsen-Gammon, and C. C. Epifanio (2005), Ensemble-based data assimilation for thermally forced circulations, *J. Geophys. Res.*, *110*, D16105, doi:10.1029/2004JD005718.

Aksoy, A., F. Zhang, and J. W. Nielsen-Gammon (2006), Ensemble-based simultaneous state and parameter estimation in a two-dimensional sea breeze model, *Mon. Weather Rev.*, in press.

Anderson, J. L. (2001), An ensemble adjustment Kalman filter for data assimilation, *Mon. Weather Rev.*, *129*, 2884–2903.

Annan, J. D., J. C. Hargreaves, N. R. Edwards, and R. Marsh (2005a), Parameter estimation in an intermediate complexity earth system model using an ensemble Kalman filter, *Ocean Modell. 8*, pp. 135–154, Hooke Inst. Oxford Univ., Oxford, England.

Annan, J. D., D. J. Lunt, J. C. Hargreaves, and P. J. Valdes (2005b), Parameter estimation in an atmospheric GCM using the ensemble Kalman filter, *Nonlinear Process. Geophys.*, *12*, 363–371.

Dowell, D., F. Zhang, L. Wicker, C. Snyder, and A. Crook (2004), Wind and temperature retrievals in the 17 May Arcadia, Oklahoma supercell: Ensemble Kalman filter experiments, *Mon. Weather Rev.*, *132*, 1982–2005.

Dudhia, J. (1993), A nonhydrostatic version of the Penn State-NCAR mesoscale model: Validation tests and simulation of an Atlantic cyclone and cold front, *Mon. Weather Rev.*, *121*, 1493–1513.

Evensen, G. (1994), Sequential data assimilation with a nonlinear quasi-geostrophic model using Monte Carlo methods to forecast error statistics, *J. Geophys. Res.*, *99*(C5), 10,143–10,162.

Evensen, G. (2003), The ensemble Kalman filter: Theoretical formulation and practical implementation, *Ocean Dyn.*, *53*, 343–367.

Gaspari, G., and S. E. Cohn (1999), Construction of correlation functions in two and three dimensions, *Q. J. R. Meteorol. Soc.*, *125*, 723–757.

Gauthier, P., and J.-N. Thépaut (2001), Impact of the digital filter as a weak constraint in the preoperational 4DVAR assimilation system of Météo-France, *Mon. Weather Rev.*, *129*, 2089–2102.

Hacker, J. P., and C. Snyder (2005), Ensemble Kalman filter application of fixed screen-height observations in a parameterized PBL, *Mon. Weather Rev.*, *133*, 3260–3275.

Hong, S.-Y., and H.-L. Pan (1996), Nonlocal boundary layer vertical diffusion in a medium-range forecast model, *Mon. Weather Rev.*, *124*, 2322–2339.

Houtekamer, P. L., L. M. Herschel, G. Pellerin, M. Buehner, M. Charron, L. Spacek, and B. Hansen (2005), Atmospheric data assimilation with an ensemble Kalman filter: Results with real observations, *Mon. Weather Rev.*, *133*, 604–620.

Lorenc, A. C. (2004), The potential of the ensemble Kalman filter for NWP–a comparison with 4D-Var, *Q. J. R. Meteorol. Soc.*, *129*, 3183–3203.

Rabier, F., H. Jarvinen, E. Klinker, J.-F. Mahfouf, and A. Simmons (2000), The ECMWF operational implementation of four-dimensional variational assimilation. I: Experimental results with simplified physics, *Q. J. R. Meteorol. Soc.*, *126*, 1143–1170.

Snyder, C., and F. Zhang (2003), Assimilation of simulated Doppler radar observations with an ensemble Kalman filter, *Mon. Weather Rev.*, *131*, 1663–1677.

Tong, M., and M. Xue (2005), Ensemble Kalman filter assimilation of Doppler radar data with a compressible nonhydrostatic model: OSS experiments, *Mon. Weather Rev.*, *133*, 1789–1807.

Zhang, F., C. Snyder, and J. Sun (2004), Impacts of initial estimate and observation availability on convective-scale data assimilation with an ensemble Kalman filter, *Mon. Weather Rev.*, *132*, 1238–1253.

Zhang, F., Z. Meng, and A. Aksoy (2006), Tests of an ensemble Kalman filter for mesoscale and regional-scale data assimilation. part I: Perfect model experiments, *Mon. Weather Rev.*, *134*, 722–736.

A. Aksoy, National Center for Atmospheric Research, P.O. Box 3000, Boulder, CO 80307–3000, USA. (aksoy@ucar.edu)

J. W. Nielsen-Gammon and F. Zhang, Department of Atmospheric Sciences, Texas A&M University, 3150 TAMU, College Station, TX 77843–3150, USA.